Supporting Information for "Fluorescence enhancement at hot-spots: The case of Ag nanoparticle aggregates"

<u>M_{Loc}, M_{Tot} and M_{sef} as a function of position in a nanoparticle aggregate on and off resonance</u>

The distributions of M_{Loc} and M_{Tot} on the surface are shown for two wavelengths (at resonance and off-resonance) in Fig S1(a) and S1(c) respectively. Note that, for simplicity, only calculations for dipolar emitters perpendicular to the surface are presented. The conclusions are the same for parallel dipoles. The fluorescence EFs, M_{SEF}, can then be deduced using Eq. 2, and their spatial distributions on the surface are shown in Fig. S1(b) and S1(d) (which are the same as Fig. 2(a-b) of the manuscript, repeated here for convenience), along with the average fluorescence EF < M_{SEF} > for each case (this is the surface average for a random distribution of molecules on the dimer). Note that these average EF cannot be directly compared to experimental values, which are strongly influenced by the polydispersity of the colloidal aggregates, i.e. distribution of size, shape, orientation, and cluster size; all influencing the relative contribution of resonant vs non-resonant clusters. However, the predicted relative average SEF EF as the distance d of the fluorophores from the surface is changed can be meaningfully compared to the experimental results (note that for a distance of d=0.2nm, the local EM theory in principle no longer applies, but it was shown in Ref. 1 that such a small distance provides EM predictions in agreement with experiment. If non-local effects were included, a larger – and more realistic – distance would then give similar results).

Fig. S1 elucidates several of the properties of a nanoparticle dimer system, and by extrapolation of more complex aggregates. On the one hand, the total decay rate and therefore modified
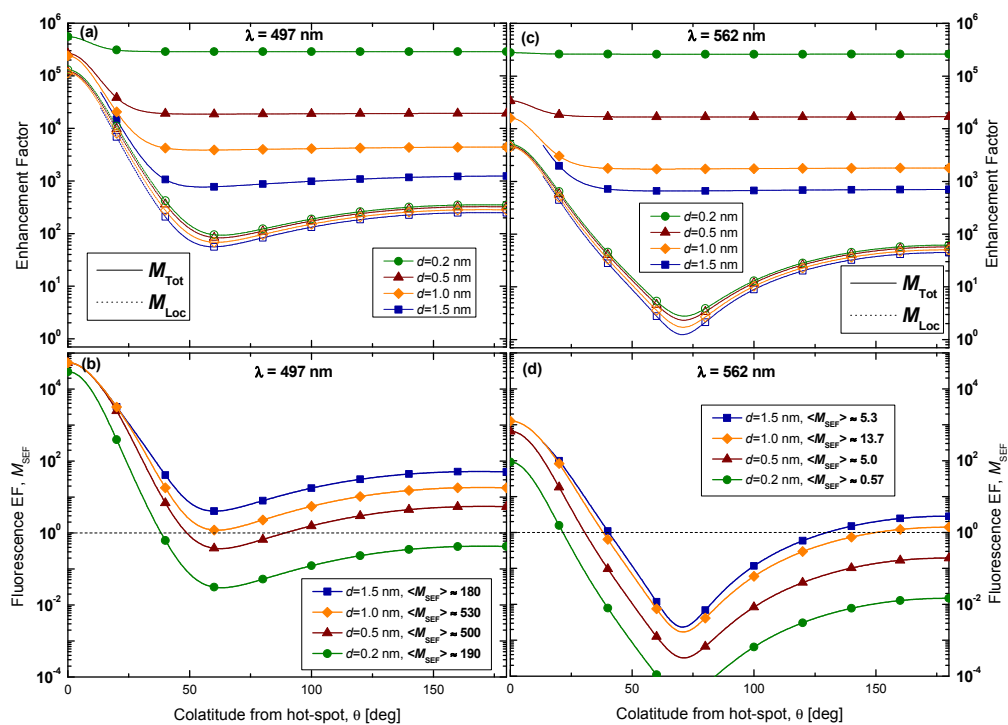
Fig. S1: Distribution of enhancement factors, M_{Loc}, M_{Tot}, and M_{SEF} (for the same dimer model as in Fig. 1) as a function of fluorophore position on the dimer surface, characterized by the colatitute (angle θ) from the hot-spot (i.e. $\theta = 0$ in the gap). Note that the longitude (ϕ) dependence is negligible. (a) and (b), left-hand side, correspond to the optimal case, where excitation is resonant, while (c) and (d), right, represent the more common case of non-optimal conditions. Four distances, d, from the surface are considered. In the case of $d = 1.5$ nm, the distribution is cut-off below $\theta = 13$ degrees because the fluorophores cannot fit in the gap while maintaining the same distance from the surface. The surface-averaged fluorescence EFs corresponding to these distributions are also given in (b) and (d).

quantum yield is extremely sensitive to distance from the surface (see Fig. S1 top), while the local field enhancement (relevant for absorption) hardly changes, at least at short distances. On the other hand, the total decay rate is independent of position (in fact it is dominated by non-radiative quenching into the metal), except at the hot-spot where its radiative component becomes important. As a result, contrary to what is generally assumed, very large fluorescence EF (up to 10^4) are predicted to occur at the hot-spot, even at ultra-short distances2. Also, fluorescence quenching is predicted everywhere outside the hot-spot at short distances (d=0.2nm). However, a distance of d=1nm is sufficient to increase the fluorescence signal of these molecules by several orders of magnitude. Moreover, the area around the hot spot that contributes to the fluorescence enhancement is increased as the distance from the surface is

increasing (going from d=0.2 to d=0.5nm and then to d=1nm). However, when this distance increases beyond half the dimer gap width, the fluorophores are no longer able to fit into the hot-spot. This causes the average enhancement to decrease as the distance from the surface increases. However, this "parking problem" is partially compensated by the beneficial effect of increasing d, and therefore even in this case, the average SEF EF decreases with distance much slower than the average SERS EF (see supporting information).

For resonant conditions (Fig. S1(a-b)), the radiative rate enhancement is so large in the hot-spot, that it dominates the total decay rate for most distances, giving very little difference between d=0.2nm and d=1nm. However, for non-optimal less-resonant conditions (Fig. S1(c-d)), the radiative rate is not enhanced as much and the total decay rate is dominated by non-radiative emission, making the effect of the distance from the surface much stronger. In polydisperse aggregates, we expect the latter situation to be relevant. Thus, we can predict, that even though for dye adsorbed to the surface, who will behave more closely to the case of d=0.2nm in Fig 2d, quenching might be observed, under similar conditions enhancement could be observed if the distance of the dye from the surface can be increased to 1-1.5nm. In the following, we therefore focus on providing an experimental demonstration of this effect in silver colloids aggregates, using dye-labelled DNA as a means to control the distance between fluorophore and surface.

Calculation of the average SERS EF of R6G

A reference standard – 0.88 nM R6G dye in ethanol, gave a reading of 2.3×10^7 counts at 560 nm after spectral calibration correction (see Figure. S2). From the shape of R6G emission curve taken from PhotochemCAD 2[3], one can calculate the ratio of the integral area to the height of the signal at 560 nm to be 66 nm. Multiplying all these numbers gives 1.7×10^9 counts×nm/nM for the total area of the fluorescence peak. For the strongest Raman peak at 1356 cm^{-1}, using 500 pM of R6G-labeled DNA and the aggregation that induces maximum SERRS signal, one can measure a total area of 2.0×10^7 counts×nm/nM. This shows that the measured Raman signal of this peak is approx. 85x smaller than the fluorescence cross section of R6G. As the total fluorescence cross section of R6G is 4.36×10^{-16} cm^2, the integrated Raman peak cross section can be approximated as 5.13×10^{-18} cm^2. Comparing this to the latest estimation of the cross section of this peak using stimulated Raman emission technique[4] (2.6×10^{-23} cm^2), we can estimate the average SERRS enhancement in this system to be 2×10^5.
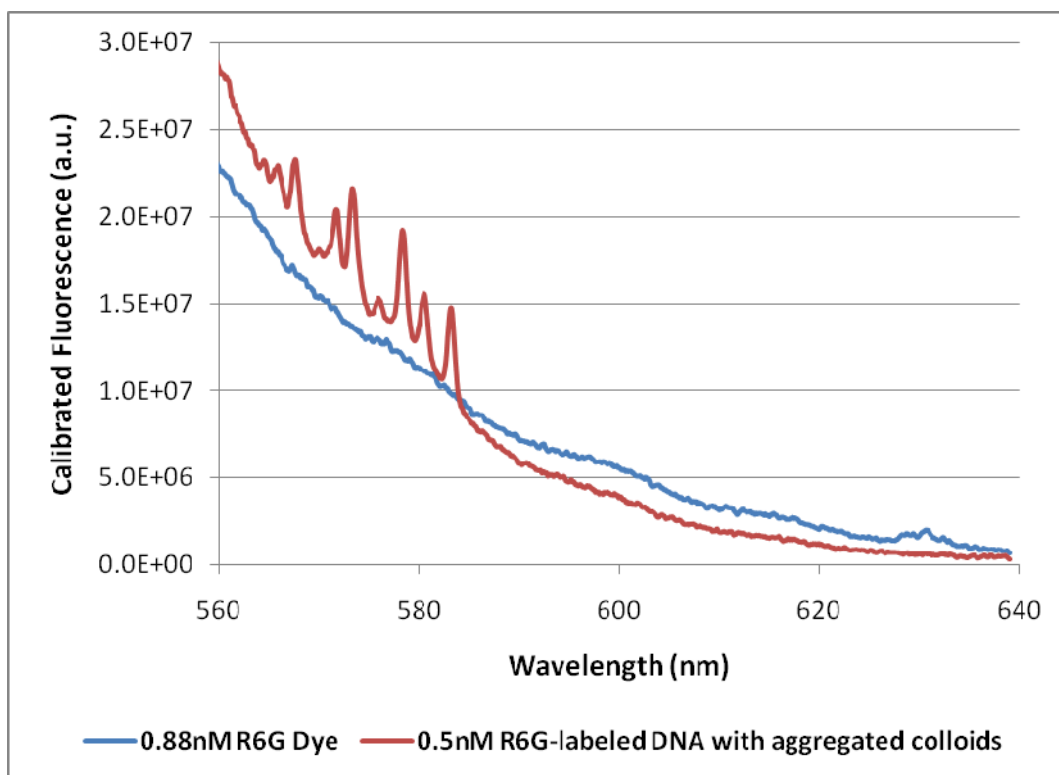
Figure S2: SERRS spectra of 500 pM R6G-labeled DNA with aggregated colloids, and Fluorescence spectra of 0.88 nM R6G dye in ethanol measured on the Raman spectrometer.

Overlap of dye spectra with the plasmon resonance peak of the Ag NPs aggregates

Figure S3(a) show the absorbance of non aggregated Ag NPs (red line) and aggregated Ag NPs (blue line). The spectrum of the aggregated particles were measured 20 sec after aggregation, which is the same time used in all SEF measurements. The aggregates absorbance peak is centered at about 530nm. The peak is wide because of the polydispersity in aggregate size and shape. Figure S3(b) shows the overlap between the absorbance spectra of the different dyes used and the wide absorbance peak of the Ag NP aggregates. The black line represent the wavelength of the laser excitataion (532 nm).

Table S1 gives the absorbance and emission peak data for the different dyes used. As can be seen all absorbance and emission frequencies are located under the central part of the plasmon peak of the aggregates.
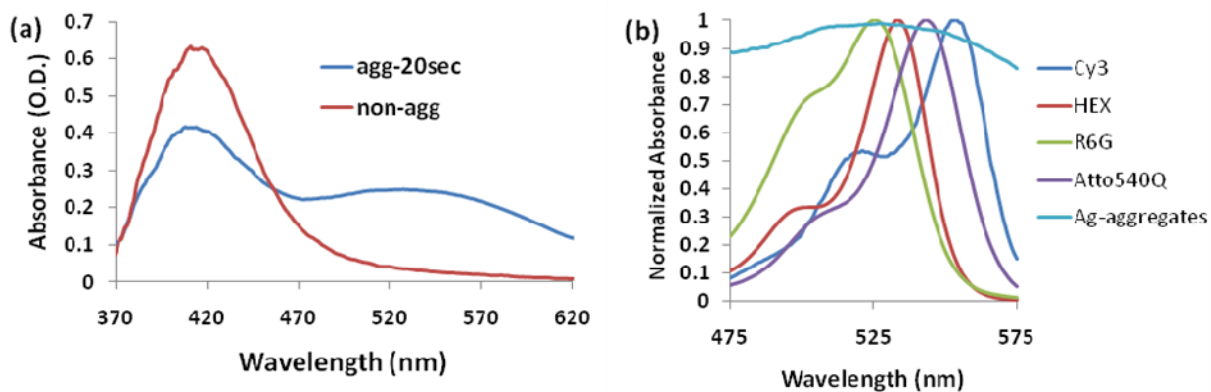
Figure S3 (a) Absorbance spectra of non aggregated (red line) and aggregated (blue line) Ag NPs. (b) Normalized absorbance spectra of the different dyes used in this study and the plasmon peak of the nanoparticle aggregates (from the measurement appearing in part (a) of this figure).

Dye	Max Abs (nm)	Max Ems (nm)
R6G	525	547
HEX	533	559
Atto 540Q	543	562
Cy3	554	566

Table S1: Absorbance and emission peak wavelength for the dyes used in this study.

Calculation of the quantum yield of dyes attached to DNA

The calculation of quantum yield for different dyes was done in a similar fashion to the calculation of the effective Raman cross section described in the previous paragraph. For any dye-labeled DNA, the total fluorescence signal at a known concentration was calculated by multiplying a measured point on the emission spectra (usually the maximal point) with the ratio of area to point height from the full fluorescence curve of the dye. This total calculated area was compared with the area of R6G dye in ethanol which has a known quantum yield of 95%. This ratio was further corrected for the ratio of extinction coefficients at 532 nm of the dye labeled DNA and R6G in ethanol.

Surface coverage of the DNA and effect of DNA concentration

In normal experiment, final concentration of DNA and Ag NPs were 500pM and 100pM respectively, giving a ratio of 5 DNA strands (29 bp, about 9.5nm fully stretched) for each 34nm diagmeter Ag NP. Even at the low salt concentration used, where the Debye length can reach 4nm, this would still give less than 20% of a full monolayer coverage. However, because spermine will bind the DNA and the nanoparticles, its effective concentration near the particles will be high, giving a much shorter Debye length than the one predicted above, and thus the DNA will amount to an even smaller percent of monolayer coverage. Figure S4 shows the fluorescence emission from experiments where 500pM of Cy3-DNA and 50pM of Cy3-DNA were used. The enhancement factor observed are x37 for the 500pM concentration and x39 for the 50pM concentration, which is only about 5% difference.
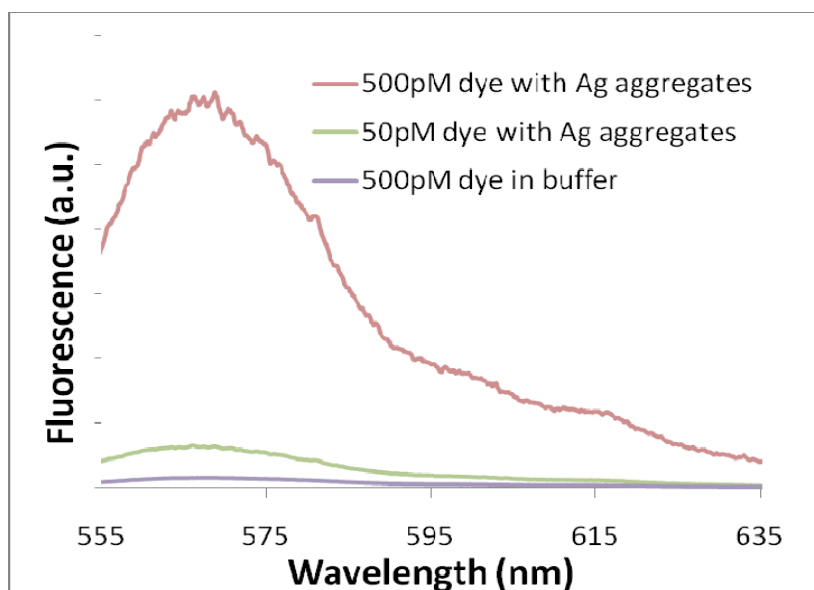
Figure S4 Fluorescence spectra of 500 pM dye-labeled DNA, in the presence (red line) and absence (purple line) of EDTA-coated silver nanoparticles (Ag-NPs), and 50pM dye-labeled DNA in the presence of Ag-NPs (green line). All experiments were conducted in a solution containing 20 μM Spermine, and 4 mM phosphate buffer pH=7.1. The NPs concentration when they were present was 100 pM. The DNA used was Cy3-DNA2.

Fluorescence enhancement of HEX-DNA2 and R6G-DNA2

The spectra used to estimate the average SEF EF of HEX-DNA2 and R6G-DNA2 are shown in

Figure. S5.
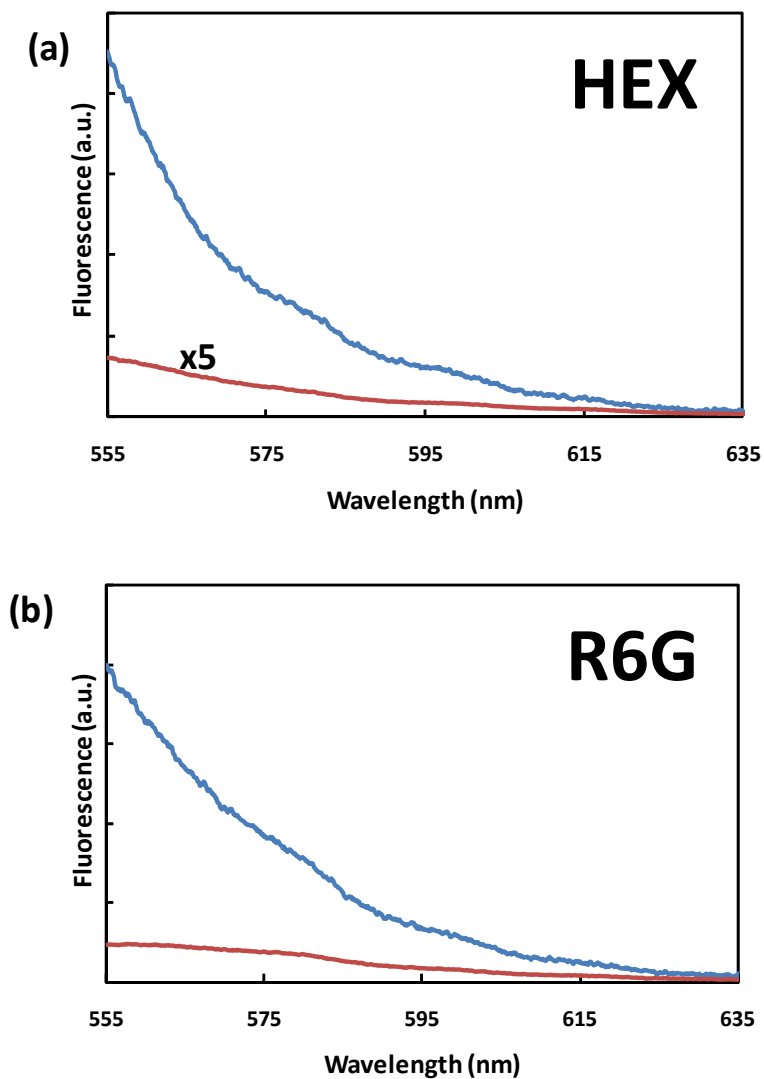
Figure S5 Fluorescence spectra of 500 pM dye-labeled DNA, in the presence (blue line) and absence (red line) of EDTA-coated silver nanoparticles (Ag-NPs). (a) HEX-conjugated to DNA-2, (b) R6G-conjugated to DNA-2. All experiments were conducted in a solution containing 20 μM Spermine, and 4 mM phosphate buffer pH=7.1. The NPs concentration when they were present was 100 pM.

Control experiments:

In order to show that only aggregated nanoparticles in the presence of dye-labeled DNA induce the enhanced fluorescence, several control experiments were performed, where one or more of the components (dye-labeled DNA, Spermine, Ag nanoparticles) were not added, but water/buffer was added instead. A typical set of measurements can be seen in Figure S6(a). Only for the HEX labeled DNA we observed a slight increase in fluorescence (x1.4) upon the addition of Ag nanoparticles (see figure S6(b)). In all other dye-DNA combinations, the dilution of dye-DNA in water gave the highest fluorescence.
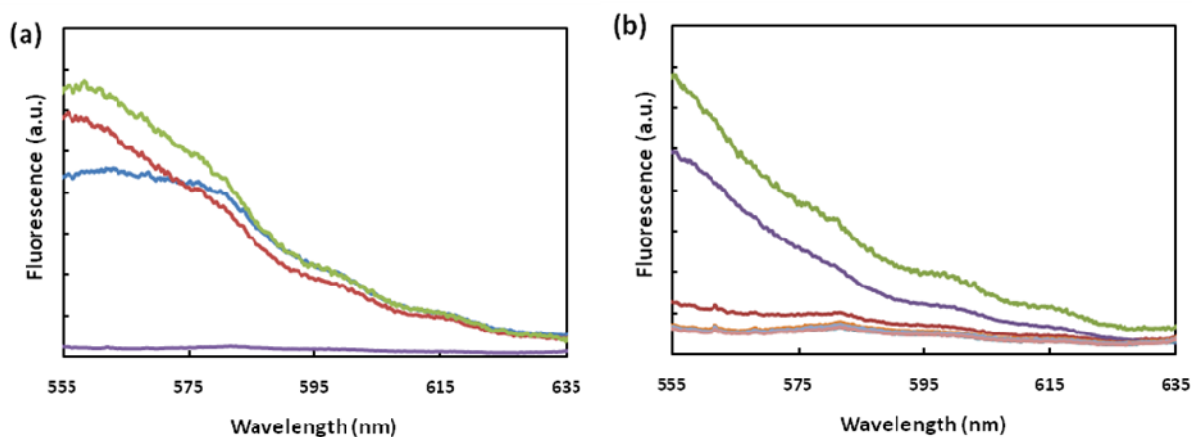
Figure S6: Fluorescence spectra of (a) 500 pM R6G-labeled DNA diluted in water (green line), 500pM R6G-labeled DNA in a solution containing 20 µM Spermine, and 4 mM phosphate buffer pH=7.1 without Ag-NPs (red line), 500pM R6G-labeled DNA in a solution containing 100pM Ag-NPs in 4mM phosphate buffer pH=7.1, but without Spermine (blue line), The background signal of a cuvette filled with triple-distilled water (violet line). (b) 500 pM HEX-labeled DNA diluted in water (violet line), 500pM HEX-labeled DNA in a solution containing 20 µM Spermine, and 4 mM phosphate buffer pH=7.1 without Ag-NPs (red line), 500pM HEX-labeled DNA in a solution containing 100pM Ag-NPs in 4mM phosphate buffer pH=7.1, but without Spermine (green line). The bottom line contains four overlapping graphs(from top to bottom): A solution containing 20 µM of Spermine, A solution containing 100pM of Ag-NPs, a solution containing both 20 µM of spermine and 100pM of Ag-NPs, triple distilled water. All the last four solutions were based on 4mM phosphate buffer and did not contain any dye-labeled DNA.

TEM microscopy:

Figure S7 shows a representative results from the TEM imaging of the nanoparticle aggregates. Both low and high resolution images are given for the same aggregates to show the nanoparticle size (apr. 34 ± 9 nm) and the interparticle distance (apr. 1-2 nm). As the aggregate is three dimentional, distances between particles can only be seen on the edges and not in the center of the aggregate.
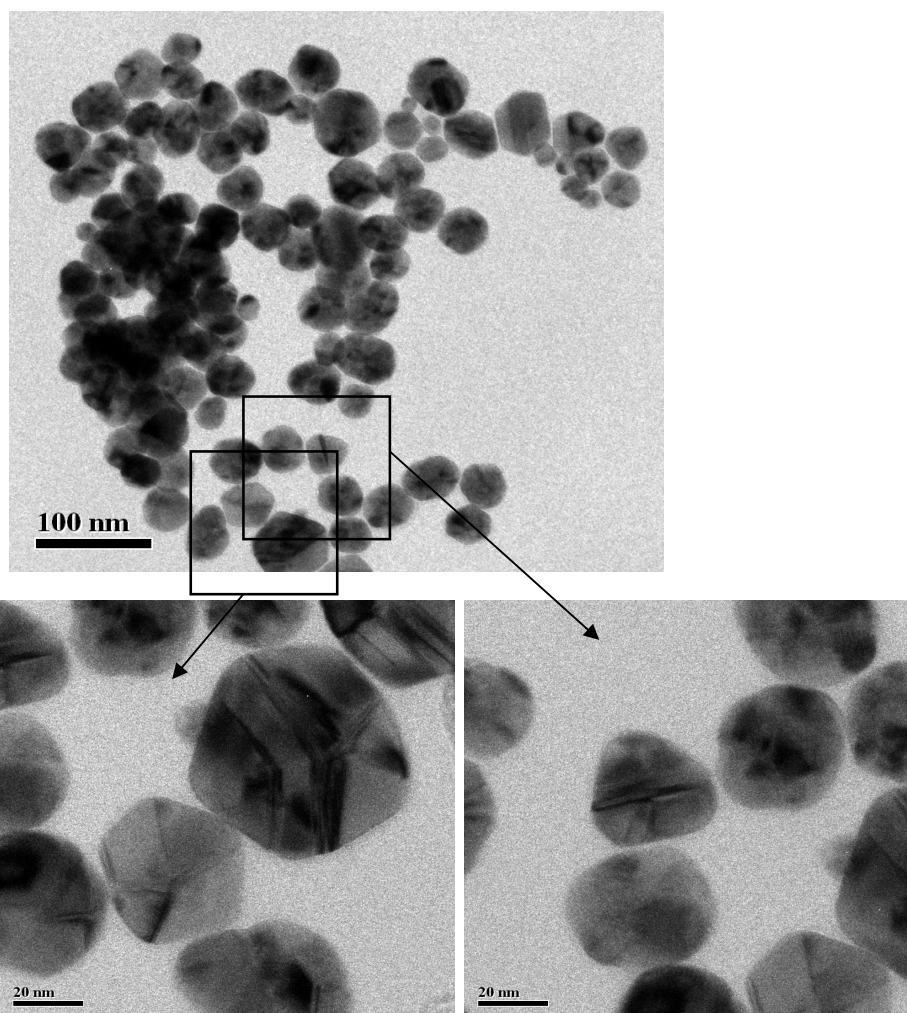
Figure S7: Transmission electron microscopy images of a nanoparticle aggregate. The top images was at x35000 and the bottom images were at x200000. Sample included 500pM R6G-labled DNA, 20 µM Spermine, and 100pM Ag-NPs in 4 mM phosphate buffer pH=7.1.

<u>Theoretical calculations of the average SERS enhancement factor</u>

Figure S7 shows the predicted distribution of SERS EF for molecules on the dimer at distances of d = 0.2, 0.5, 1, 1.5, and 2 nm from the metal surface. The geometrical parameters have been chosen as in the main text as the best estimates for our experiments: Ag sphere radius is 17 nm, gap between spheres is 2nm, embedding medium is water. The excitation wavelength is then chosen as the resonant wavelength for the particular structure here (497 nm), and the incident polarization is along the dimer axis. Similar results are obtained at 532 nm or 562 nm excitation or with other incident polarizations, only with smaller SERS EFs (see for example Table S1). Note that we are only interested in relative changes in the SERS EF distribution. The absolute value of the predicted SERS EF is irrelevant here, since predicting it would require averaging over the polydispersity of the aggregates and over their orientation[5].

Fig. S8 and Table S2 highlight several important aspects of the SERS EF distribution and average at a hot spot:

- The average SERS signal is dominated by molecules in a very small area around the hot-spot, typically less than 1% of the total area[5].

- The SERS intensities are not very sensitive to the distance from the surface at short distances (as opposed to the case of SEF, see main text).

- -However, as the molecules move away from the surface (and we assume that they must also remain the same distance away from the second sphere surface), they can no longer fit into the gap between the two colloids where the SERS EF is highest. This "parking problem" has a much more dramatic impact on the average SERS EF as the simple distance dependence of the SERS EF. For example, although the SERS EF at a given point

drops by a factor of only approx 1.4 when going from d = 1 nm to d = 1.5 nm, the average

SERS EF drops by a factor of more than 10, simply because the points of highest

enhancements at the hot-spot are no longer accessible to the molecule. It drops by another

factor of 10 when going to d = 2 nm.
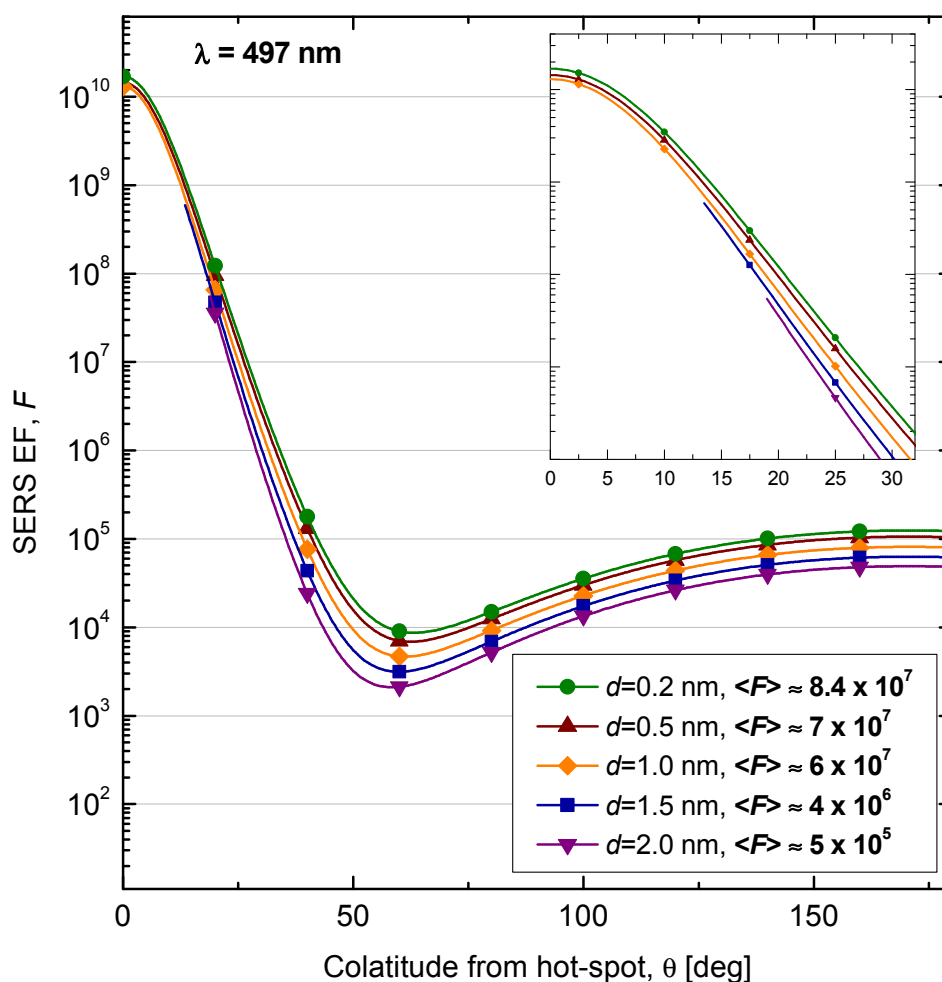
Figure S8: SERS enhancement factor, F, as a function of angle and distance from the surface of a silver dimer (34 nm diameter particles, 2 nm interparticle distance, embedded in water). For $d > 1$ nm, the distributions are cut-off at the point where the molecule can no longer fit in the gap while maintaining the same distance from the surface ("parking problem"). The corresponding average SERS EF are indicated in the legend. Although the punctual SERS EFs do not decrease substantially with d, the average SERS EFs drop sharply for $d > 1$ nm as a result of the parking problem. The inset shows a zoom of the region around the hot-spot.

Table S2: Summary of predicted surface-averaged SERS EF, $<F>$ (calculated using Eq. 1 of the main text) for the same dimer structure as studied in Figure. S3, at three different excitation wavelengths.

Excitation wavelength	497 nm	532 nm	562 nm
d=0.2nm	8.4×10^7	1.5×10^6	1.6×10^5
d=0.5nm	7×10^7	1.3×10^6	1.3×10^5
d=1.0nm	3×10^7	1.1×10^6	1.1×10^5
d=1.5nm	4×10^6	1.0×10^5	1.3×10^4

Reproducibility of the fluorescence measurement in the presence of silver nanoparticle aggregate

In fig 6 of the main text, we claim that the spread in the measurement of the fluorescence enhancement is lower than the relative size of the marker used in the graph. This might seem counter-intuitive given the random nature of the aggregation process we employ to drive the fluorescence enhancement. However, it can be understood based on the fact that the measurement device we employ (R3000) uses a detection volume of 100um diameter. Therefore in this volume there are thousands of aggregates, that while they are not all the same size, their statistical average is determined by the initial volumes/concentration of the nanoparticle and aggregating agent solution used. Therefore, as long as we repeated mixing the same volume and same concentrations, the results repeated themselves with a very small coefficient of varience (CV) – see figure S9, black curves. However, it should be noted that the aggregating is a dynamic process, and therefore for reproducibility, the time of the measurement after the mixing is also important. As can be seen in figure S9, red curve, when measuring after 10% longer time (compared to t=20s which gave the optimal results), the fluorescence was 3% less.
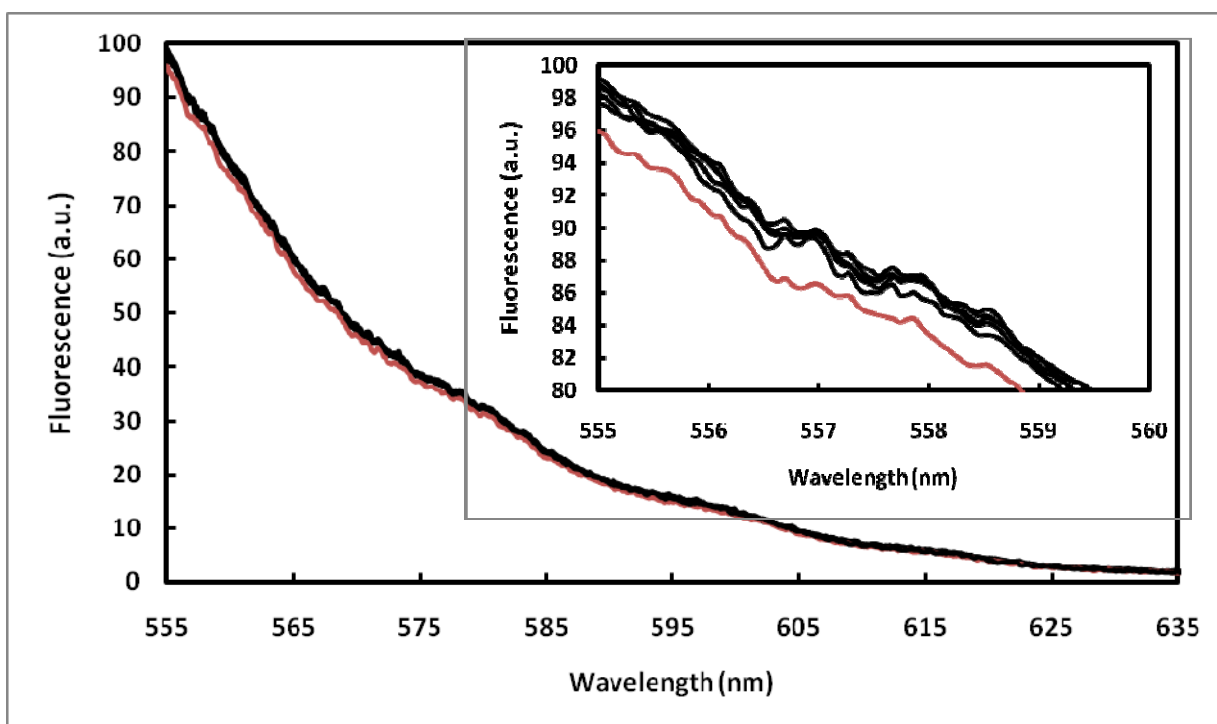
Figure S9: Fluorescence spectra of 500 pM R6G-DNA1 in the presence of EDTA-coated silver nanoparticles. The black curves are 5 repeates all measured 20s after mixing. The red curve is a 6th repeat mesured after 22s. In the insert appears a magnification of the same data from the top left corner of the main graph. All experiments were conducted in a solution containing 20 μM Spermine, and 4 mM phosphate buffer pH=7.1. The NPs concentration was 100 pM.

References:

1   C. M. Galloway, P. G. Etchegoin and E. C. Le Ru, *Phys. Rev. Lett.*, 2009, **103**, 063003.
2   E. C. Le Ru, P. G. Etchegoin, J. Grand, N. Felidj, J. Aubard and G. Levi, *J. Phys. Chem. C*, 2007, **111**, 16076-16079.
3   M. D. James, T. Masahiko and S. L. Jonathan, *Photochem. Photobiol.*, 2005, **81**, 212-213.
4   S. Sangdeok, M. S. Christina and A. M. Richard, *ChemPhysChem*, 2008, **9**, 697-699.
5   E. C. Le Ru, E. Blackie, M. Meyer and P. G. Etchegoin, *J. Phys. Chem. C*, 2007, **111**, 13794-13803.